

Crack propagation simulation of concrete with the regular triangular lattice model

Byung-Wan Jo[†]

Department of Civil Engineering, Hanyang University, Korea

Ghi-Ho Tae[‡]

Department of Civil Engineering, Bucheon University, Korea

Erik Schlangen[†]

Department of Civil Engineering, Delft University Technology, Netherlands

Chang-Hyun Kim^{‡†}

Department of Civil Engineering, Hanyang University, Korea

(Received October 6, 2004, Accepted March 28, 2005)

Abstract. This paper discusses 2D lattice models of beams for simulating the fracture of brittle materials. A simulation of an experiment on a concrete beam subjected to bending, in which two overlapping cracks occur, is used to study the effect of individual beam characteristics and different arrangements of the beams in the overall lattice. It was found that any regular orientation of the beams influences the resulting crack patterns. Methods to implement a wide range of Poisson's ratios are also developed, and the use of the lattice to study arbitrary micro-structures is outlined. The crack patterns that are obtained with lattice are in good agreement with the experimental results. Also, numerical simulations of the tests were performed by means of a lattice model, and non-integer dimensions were measured on the predicted lattice damage patterns.

Keywords: lattice model; simulation; overlapping cracks; crack pattern.

1. Introduction

Since concrete is a highly heterogeneous material and concrete cracking is a localized phenomenon (resulting in stress redistributions during cracking), the implementation of concrete cracking into finite element codes is not straightforward (Bazant 1995). Iterative calculation techniques have to be adopted for correct predictions of the highly non-linear material behavior (Walraven 1980). In this respect two main approaches to modeling concrete can be distinguished, namely by continuum or

[†]Professor

[‡]Professor, Corresponding Author, E-mail: civilianho@dreamwiz.com

^{‡†}Graduate Student

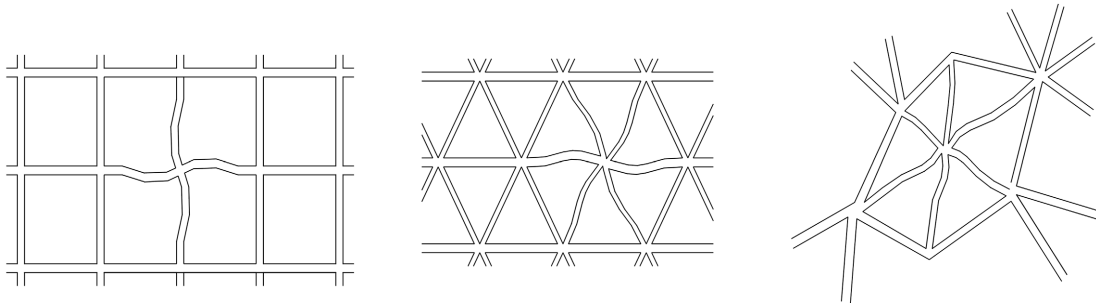


Fig. 1 Lattice types: regular square lattice (a), regular triangular lattice (b) and random lattice(c)

discrete methods. When a continuum model is adopted for “predicting” fracture processes in concrete, the macro-level is usually chosen as the level of modeling. When, on the other hand, the material’s micro-level is addressed, and the material is treated as three phase material (aggregate, matrix and interface between matrix and aggregates), a brittle constitutive relation seems satisfactory. In spite of the individual elastic-brittle behavior of the material constituents, non-linearity will be observed at the macro-level (Carpinteri 1994). In the model presented in this paper, the second (discrete or lattice) approach is used for modeling concrete cracking at the meso-level. In such a model the material is discretized by a network of beams or trusses, and cracking is modeled by removing a beam from the mesh. Through the years, considerable attention has been given to lattice models. Lattice type models were first developed in theoretical physics. The original model proposed by Herrmann incorporated a regular square lattice illustrated in Fig. 1a. For simulating concrete fracture the regular triangular lattice (Fig. 1b) was proposed by Schlangen and Van Mier (1993). A random lattice, proposed by Moukarzel and Herrmann, has been used for similar purposes. In this random lattice, the connectivities of the beams are determined by the Voronoi construction of a set of nodes. The random lattice is illustrated in Fig. 1c. Most of the simulations of concrete fracture presented in this paper were carried out with the regular triangular lattice that was mentioned before.

2. Principle of the lattice model

In the adopted lattice model directly beam elements with three degrees of freedom are used. The constitutive relation of an element is linear-elastic, and the stress in an element is calculated as a combination of the normal force and the bending moments acting on the element (Vervuurt 1997). This “effective” stress causes failure as soon as the strength of the beam element is exceeded. Because of the linear-elastic behavior of the lattice, the failure load of a beam is calculated within a single step of a finite element analysis. This procedure of loading the mesh and consequently removing an element is repeated until complete failure of the lattice has been obtained. In order to reduce the computational effort, generally only the area of the specimen where cracks are expected to grow is modeled with a lattice (Van Mier 1995). The remainder of the specimen is modeled with continuum elements. The simulations presented in this paper are carried out with the finite element package DIANA, mainly because of the availability of several types of continuum elements besides the beam elements required for the lattice. At the boundary between lattice and continuum elements,

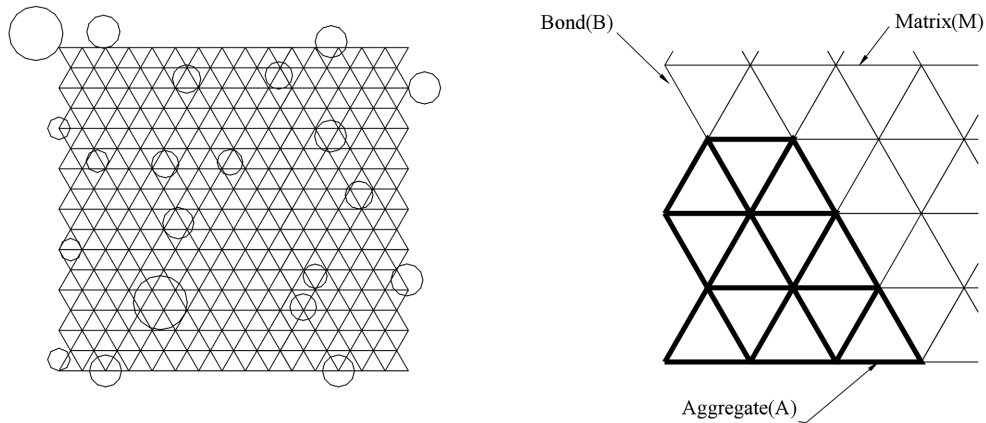


Fig. 2 Aggregate structure projected on top of a lattice (a) definition of aggregate, bond and matrix beams (b)

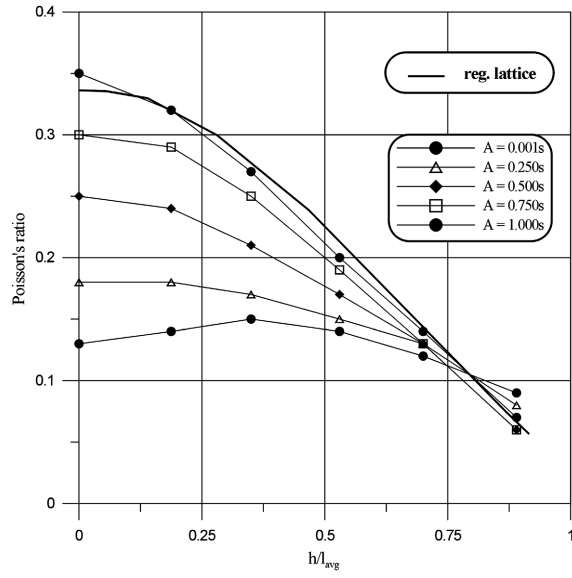
the beam nodes are the nodes of the continuum elements. In order to reduce the computer time, the lattice model is currently being implemented as a “special” module in the DIANA finite element code. Although each individual element in a lattice fails brittle, the (global) softening behavior of heterogeneous materials like concrete can be simulated with the model. When a regular lattice (Fig. 1b) is used, heterogeneity has to be implemented in the model in order to obtain realistic crack patterns observed in concrete experiments. Heterogeneity is introduced by varying the Young’s modulus and the strength of the beam elements. Considering the material structure of concrete, a realistic strength and stiffness distribution strength and stiffness of the distinctive phase are assigned to the beams falling inside the aggregates (A), in the matrix (M) or at the interfacial zone between the aggregate and the matrix (bond, B).

3. Parameter determination

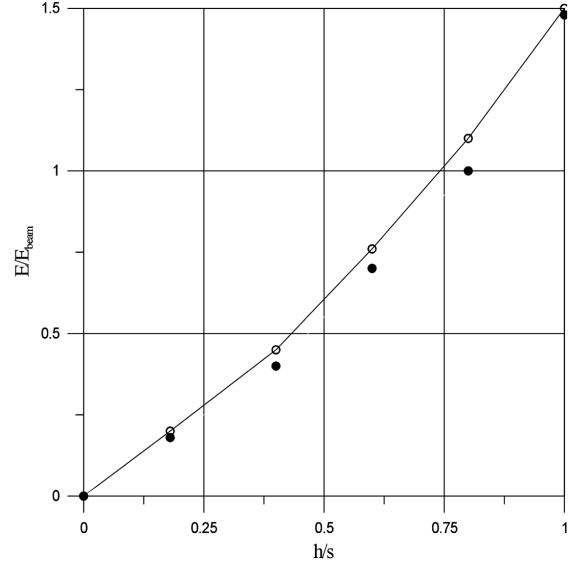
The advantage of the lattice model is that is a simple and transparent model. Only a few, single valued parameters are required in the model. These parameters can be divided in two groups: i.e., parameters according to the global elastic behavior of the mesh and parameters needed in the fracture law.

3.1. Parameters related to the elastic behavior

To describe the global elastic behavior of the lattice, the Young’s modulus (E) and Poisson’s ratio (ν) of the material which is to be modeled are available as input. They have to correspond to the global behavior of the lattice, which can be adjusted by changing the geometrical properties (height h and thickness t) and the global Young’s modulus of the beams (E_{beam}). For two dimensional simulations, it seems obvious to choose the beam thickness equal to the thickness of the simulated specimen. When a regular lattice is adopted, the remaining beam properties (h and E_{beam}) can be determined in a very straightforward manner, since the Poisson’s ratio of the lattice is directly related to the height over length ratio of the beams. For a regular triangular lattice without particle



(a)



(b)

Fig. 3 Relation between ν and h/l_{avg} for a triangular lattice with varying P_k

overlay and consisting of prismatic beams it was found that:

$$\nu = \frac{1 - \frac{12l}{Al^2}}{3 + \frac{12l}{Al^2}} = \frac{1 - \left(\frac{h}{l}\right)^2}{3 + \left(\frac{h}{l}\right)^2} \tag{1}$$

where l is the length of a beam in modeling, $l = 1/12t \cdot h^3$, and A is the cross sectional area ht .

This function is shown graphically in Fig. 3, with the results for the lattice with varying P_k (the ratio of the aggregate volume to the total volume of the concrete). The Poisson's ratios for the lattices given in Fig. 3a are the average values resulting from calculations on 175 meshes measuring 50×50 nodes. When the height of the beams is fixed, the local Young's modulus of the beams (E_{beam}) can be determined from the global stiffness of the lattice, which has to be coincident with the stiffness of the material that is modeled. In Fig. 3b the relation between the ratios E/E_{beam} and h/s is shown by the five different value of the A . The stiffness of the lattice can be varied by changing the Young's modulus of the beams. The values of the ratios, however, must be kept constant in order to maintain a linear relation between E and E_{beam} .

3.2. Fracture law parameters

Next to the parameter related to the global elastic behavior of the mesh, parameters related to fracture law are required. After generating the mesh and assigning the elastic properties to the beams, the load is applied and a linear elastic analysis is performed. Then the parameter related to the global elastic behavior of the mesh, parameters related to the fracture law is required. Cracking is obtained by removing one beam from the mesh in each step of a lattice analysis. The choice of the beam which has to be removed from the mesh is based on a very simple fracture law in which the "effective" stress (f) is calculated following:

$$f_{eff} = \beta \cdot \left(\frac{F}{A} + \alpha \frac{|M_i - M_j|_{max}}{W} \right) < f_t \quad (2)$$

where F is the normal force in the beam, A is the cross sectional area, M_i and M_j are the moments in the two respective nodes of the beam and $W = 1/6 \cdot b \cdot h^2$ is the sectional moment of the beam. The parameter α is used to control the fracture mode: bending can either play a dominant

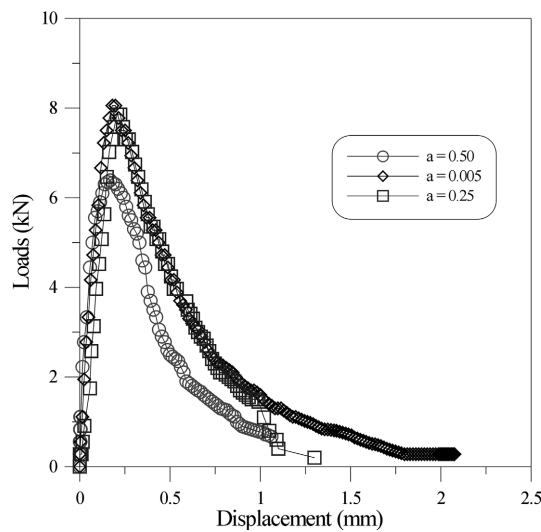


Fig. 4 Load-deformation curves for three simulations with different values for α

or a restricted role. Changing α affects the tail in the stress-deformation curve. However, the influence of changing α is small. In Fig. 4 three curves for three different values for α are shown. The curves have been scaled in such a way that the peak loads are equal. A small α gives a long tail in the stress-deformation response, whereas a large α results in more brittle global behavior.

The parameter β is implemented for fitting the curve, after the simulation is carried out, such that the maximum load in the simulation is equal to the maximum load in the experiment. When the effective stress of a particular beam exceeds its tensile strength f_t , brittle fracture is simulated by instantaneously removing the beam element from the lattice. This implies that an energy package equal to $U_e = f_t^2 / 2E$ is released from the structure at each element removal (Van Mier 1999).

The Young's moduli of aggregate, matrix and bond zones are given realistic values determined in

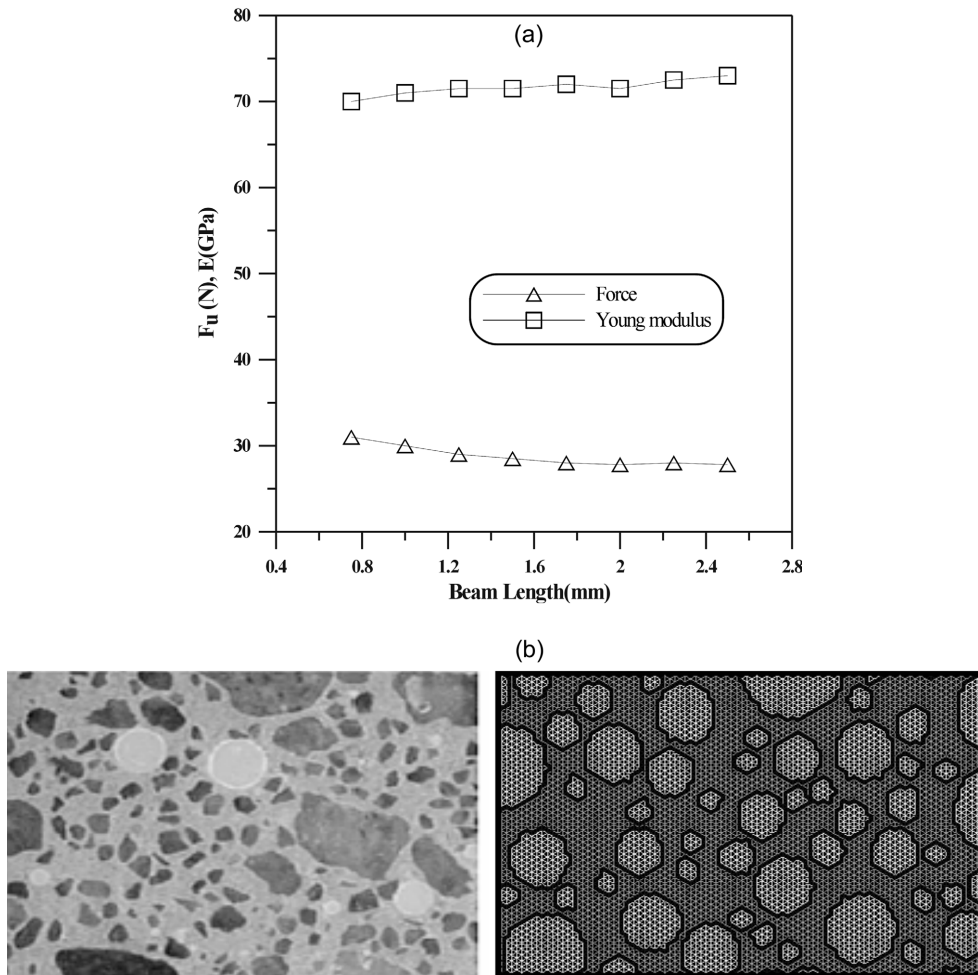


Fig. 5 (a) Calculated ultimate strength and global Young's modulus $2 = d = 8$, $P_k = 0.75$, (b) A compared mortar particle and modeling of $P_k = 0.75$ value

experiments, whereafter the section dimensions are adjusted. For fracturing the beam elements a different threshold for the tensile strength is specified for beams falling in the three different material phases. The ratios of these strength values are of importance. They are $f_{tM}/f_{tA} = 5/10$ and $f_{tB}/f_{tM} = 1.25/5$. These values imply a high strength aggregate in a lower strength matrix, but the weakest link is formed by the interfaces. In all analyses $\alpha = \text{constant} = 0.005$, which yields the development of a long tail in the load-deformation diagram.

3.3. Particle distribution and properties

Fig. 5(a) shows that the force that can be carried by the global lattice hardly varies with beam length. This indicates that, for the present example with $P_k = 0.75$, failure is governed by the weakest elements, i.e., the bond beams, as will become clear further on. Also, Fig. 5(b) shows that relationship modeling of $P_k = 0.75$ value and mortar particles.

Fig. 6 shows the variation of the different phases ‘matrix’, ‘bond’ and ‘aggregate’ as a function of the beam length. A parameter P_k in the distribution function refers to the aggregate volume as a ratio to the total volume. Realistic for concrete are values of P_k around 0.75. Fig. 6(a) shows that the bond fraction approaches an asymptotic value with increasing beam length. At a certain moment only the largest particles are present in the mesh. The number of such large-sized particles is limited in the fuller distribution that was used. In Fig. 6(a) the phase fractions are shown for a fuller-type distribution for varying P_k values. The beam length was equal to $l = 1$ mm. The actual $P_{k,lat}$ (defined as the number of aggregate beams relative to the total number of beams deviates from the theoretical values P_k used for generating the particle structures as mentioned before). For example for $P_k = 0.1, 0.4, 0.7$ and 1.0 , the actual values were $P_{k,lat} = 0.03,$

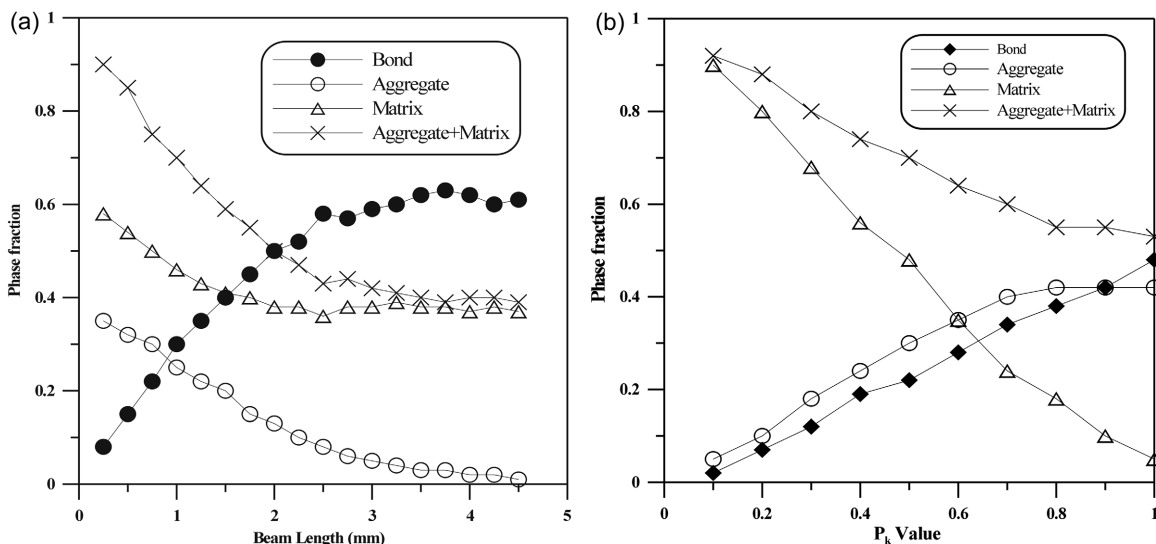


Fig. 6 (a) Phase fractions of bond, matrix and aggregate beams as a function of beam length, (b) Fraction of bond, matrix and aggregate phases with varying P_k

0.19, 0.34 and 0.48 respectively, as is shown by the circles in Fig. 6(b). The actual value of $P_{k,lat} = 0.48$ is the maximum aggregate fraction that can be obtained for a system with round aggregates, encircled with an interfacial transition zone of constant thickness (one beam length), for a beam length $l = 1$ mm. The amount of matrix needed is bound by a minimum value, since all open space between the spherical aggregates must be filled. With increasing P_k , Fig. 6(b) shows an increase of both the bond and aggregate fractions. Around $P_k = 0.6$, the number of bond beams exceeds the number of matrix beams, indicating a larger probability for exceeding the percolation threshold of the bond beams.

4. Application of the lattice model

In order to apply to the lattice model, the model has been used for experiment test. The main purpose of these calculations was to validate the model by means of comparing the numerical results to those of experiments. In Table 1 the values of the input parameters giving the best fit with the experiment are listed. A lattice with beam elements is loaded in bending. The Young's modulus

Table 1 Input parameters for simulations

Beam elements	$l = 5/3$ mm	$h = 0.68 l$	$b =$ Specimen thickness
Strengths	$f_{t,A} = 10$ MPa	$f_{t,M} = 10$ MPa	$f_{t,B} = 10$ MPa
Stiffness	$E_A = 70$ GPa	$E_M = 25$ GPa	$E_B = 25$ GPa
	$\alpha = 0.005$	$\beta = 2.0$	

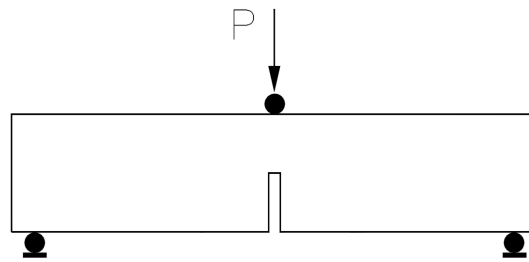


Fig. 7 Three-point bending test specimen

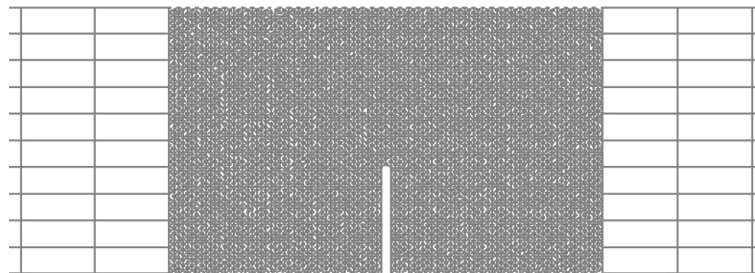


Fig. 8 Three-point bending specimen and lattice analysis modeling

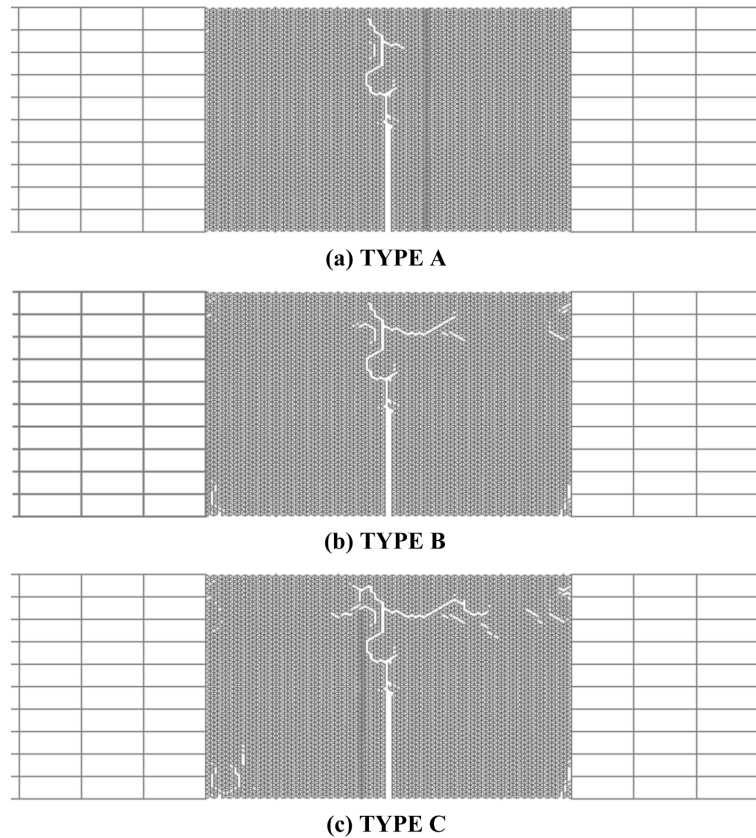


Fig. 9 Simulation of a bending test on a specimen using different lattice element number

Table 2 Overview of the lattice types compared in a bending test

Lattice type	Abbreviation
Triangular lattice with particle structure (Number of node and element 672, 1283)	TYPE A
Triangular lattice with particle structure (Number of node and element 2542, 4966)	TYPE B
Triangular lattice with particle structure (Number of node and element 10004, 19772)	TYPE C

E of the beams is taken equal to the stiffness of the material. The thickness b of the beams is taken equal to the thickness of the material. These values are chosen such as to get an easy adjustment if fracture in materials with a different stiffness or specimens with a different thickness are to be simulated. The notched three-point bending specimen and lattice modeling of the specimen are shown in Fig. 7 and Fig. 8

Also, to get an insight in the behavior of these different lattice types a comparison was made by simulating the behavior of a single notched specimen under three point bending test. The area of the

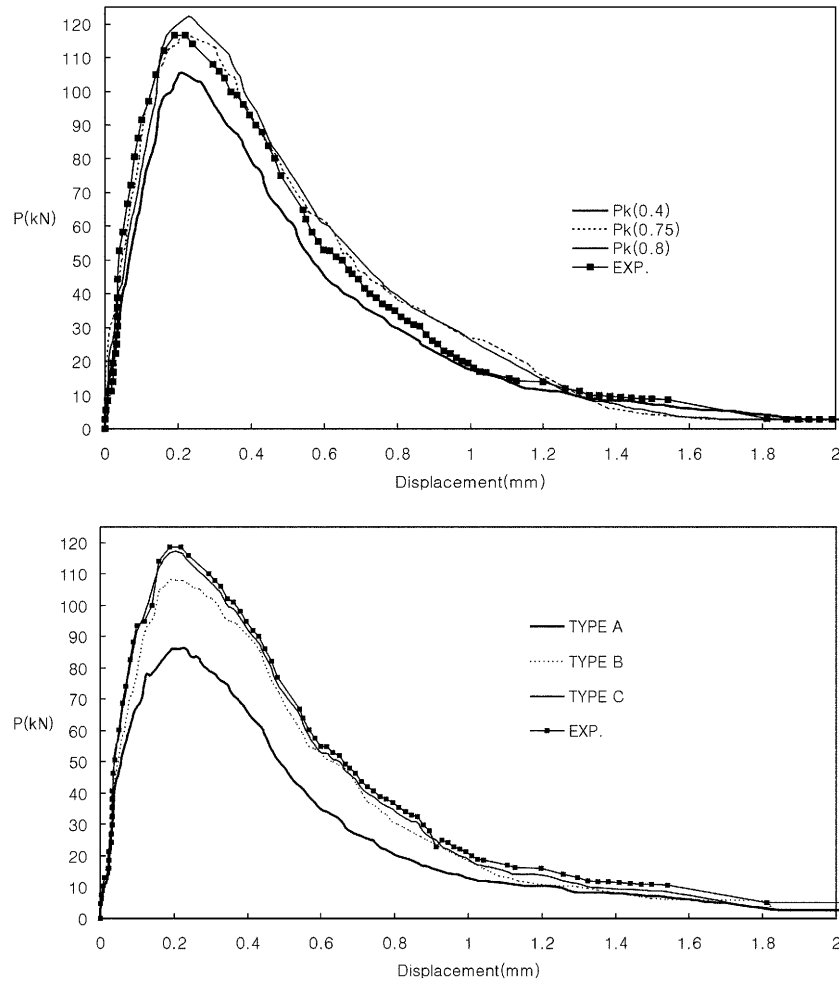


Fig. 10 Compare P - δ of analyzed lattice types to experiment specimen

specimen that was used to control the deformations in the laboratory test was modeled with three different lattices, denoted Type A to C in Table 2.

In Fig. 9(a)~(b) the cracks in the lattice part of the specimen are shown at almost the same crack mouth opening displacement (CMOD). Because of the presence of a grain overlay in the mesh, micro-cracks develop in the bond zones around the grains, apart from the continuous cracks in the cement matrix. Since this mechanism resembles the actual fracture process in concrete, TYPE B seems most suitable for modeling this material.

The load-midspan deflection curves of the lattice element types are shown in Fig. 10(a)~(d), respectively. The displacement given in the figure is measured at the load application point. Three curves correspond to the three types in each size group, which differ only by the random distribution of the equal amount of aggregates.

5. Discussion and conclusions

This paper discussed 2D lattice model for fracture simulations. In this paper, models with various types of elements can be found. The equations for the network models with these different elements are all discretizations of different continuum equations. The square lattice model has been successfully used to simulate the complete load-deformation response of notched three point bending beams. For fracture the results that are obtained strongly depend on the chosen element type. Beam elements with three degrees of freedom per node give the best agreement with experimentally obtained crack patterns. In simulations with different P_k (aggregate size) is 0.75, realistic crack patterns are also obtained. However the crack patterns that are simulated are not complicated. Bending tests are simulated in which a straight crack surrounded by microcracks developed. In Fig. 8 of this paper, it is shown that if the crack pattern is more complex, and the cracks are curved, elements with three degrees of freedom are necessary. The shape or orientation of the beams in a lattice also influences the simulated crack patterns, with the cracks tending to follow the mesh lines. Cracks in such a lattice develop perpendicular to the maximum tensile stress in the specimen and are independent of the mesh orientation. It is not known whether sets of A s and I s that are all positive exist or not. However, the small fraction of beams that have negative values of A and/or I do not adversely affect either the computed elastic moduli or simulated fracture patterns.

References

- Walraven, J. C. (1980), "Aggregate interlock: A theoretical and experimental analysis", Ph. D. thesis, Delft University of Technology.
- Bazant, Z. P. (1984), "Size effect in blunt fracture: concrete, rock, metal". *J. Eng. Mech.*, ASCE **110**, 518-535.
- Karihaloo, B. L. (1985), *Fracture Mechanics and Structural Concrete*. UK: Addison Wesley Longman, 151.
- Bazant, Z. P. and Pfiffner, P. A. (1988), "Determination of fracture energy properties from size effect and brittleness number", *ACI Mater J.*, **111**, 463-480.
- Schlangen, E. (1993), "Experimental and numerical analysis of fracture processes in concrete", Ph. D. Thesis, *Delft University of Technology*, 62-65.
- Carpinteri A. (1994), "Fractal nature of material microstructure and size effects on apparent mechanical properties", *Mech. Material*, **18**, 89-101.
- Van Mier, J. G. M., Schlangen, E. and Vervuurt, A. (1995), "Lattice type fracture models for concrete", In *Continuum Models for Materials with Microstructure*, H. B. Muhlihaus(ed.). John Wiley & Sons Ltd., 341-377.
- Vervuurt, A. H. J. M. (1997), "Interface fracture in concrete", Ph. D. thesis, Delft University of Technology.

Notation

P_k	: ratio of the aggregate volume to the total volume of the polymer concrete
A	: cross section area
l	: length of a beam in modeling
α	: fracture parameter
β	: scaling factor, shear retention factor
E_A, E_B, E_M	: Young's modulus aggregate, bond, matrix
F	: normal force
f_b	: bending strength

f_c : compressive strength
 f_t : tensile strength
 $f_{t,A}, f_{t,B}, f_{t,M}$: tensile strength aggregate, bond, matrix
 P_{pre} : prescribed external load

CC